

Transition-State Structure in the Yeast Alcohol Dehydrogenase Reaction: The Magnitude of Solvent and α -Secondary Hydrogen Isotope Effects[†]

Katherine M. Welsh,[‡] Donald J. Creighton,[§] and Judith P. Klinman*

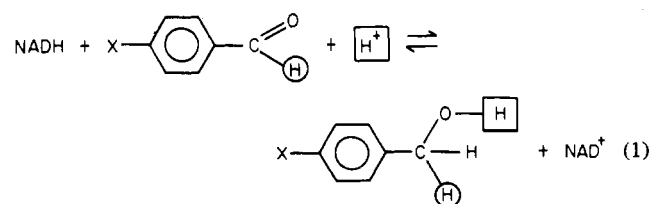
ABSTRACT: Solvent and α -secondary isotope effects have been measured in the yeast alcohol dehydrogenase reaction, under conditions of a rate-limiting transfer of hydrogen between coenzyme and substrate. Determination of catalytic constants (at saturating concentrations of substrate and coenzyme) in H₂O and D₂O as a function of pH(D) has allowed the separation of solvent effects on pK_a from k_{cat} : $\Delta pK_a = pK_D - pK_H = 0.02-0.21$, $k_{H_2O}/k_{D_2O} = 1.20 \pm 0.09$ in the direction of *p*-methoxybenzyl alcohol oxidation, and $k_{H_2O}/k_{D_2O} = 0.50 \pm 0.05$ and 0.58 ± 0.06 for *p*-methoxybenzaldehyde reduction by NADH and [4-²H]NADH. The small effect of D₂O on pK_a , which contrasts with the common observation that $\Delta pK_a \approx 0.4-0.6$, is tentatively assigned to ionization of an active-site ZnOH₂. The near absence of an isotope effect on k_{cat} in the direction of alcohol oxidation rules out a mechanism involving concerted catalysis by an active-site base of hydride transfer. In the direction of aldehyde reduction, the observation of inverse isotope effects on k_{cat} is concluded to reflect dis-

placement of zinc-bound water by substrate to form an inner-sphere complex, subsequent to the E·S complex. Equilibrium α -secondary isotope effects, measured as a frame of reference for kinetic values, indicate $K_H/K_T = 1.33 \pm 0.05$ and 1.34 ± 0.09 for the oxidation of [1(*S*)-³H]benzyl alcohol and *p*-methoxy[1(*S*)-³H]benzyl alcohol, respectively. Kinetic α -secondary isotope effects are within experimental error of equilibrium values, $k_H/k_T = 1.34 \pm 0.07$ and 1.38 ± 0.02 for [1(*S*)-³H]benzyl alcohol and *p*-methoxy[1(*S*)-³H]benzyl alcohol oxidation, respectively. The near identity of kinetic and equilibrium α -secondary isotope effects in the direction of alcohol oxidation implicates a transition-state structure which resembles aldehyde with regard to bond hybridization properties. This result contrasts sharply with previously reported structure-reactivity correlations, which implicate a transition-state structure resembling alcohol with regard to charge properties. The significance of these findings to the mechanism of NAD(P)H-dependent redox reactions is discussed.

Among NAD(P)-dependent enzymes, alcohol dehydrogenases are distinguished by the successful kinetic isolation of bond rearrangement from protein isomerization and product release steps. Although coenzyme dissociation normally limits V_{max} for horse liver alcohol dehydrogenase [Brändén et al. (1979) and references cited therein], Plapp and co-workers (Dworschack & Plapp, 1977) have shown that chemical modification of lysine side chains leads to a rate-limiting transfer of hydrogen between coenzyme and substrate under steady-state conditions. In addition, a large number of investigators have employed transient kinetic techniques to examine the interconversion of ternary complexes under single turnover conditions [e.g., Bernhard et al. (1970), Shore & Gutfreund (1970), Hardman et al. (1974), Kvassman &

Pettersson (1976), and references cited in Klinman (1980)].

In the case of alcohol dehydrogenase from yeast, the reduction of aromatic aldehydes by NADH is characterized by large primary hydrogen isotope effects (Klinman, 1972). A comparison of the magnitude of isotope effects and ρ values for benzaldehyde reduction by NADH to benzyl alcohol oxidation by NAD⁺ leads to the conclusion of a single rate-limiting hydrogen transfer for a series of aromatic aldehyde/alcohol substrates (Klinman, 1976). These studies have facilitated further investigations of the chemical reaction, and in this paper we report solvent and α -secondary hydrogen isotope effects for the benzaldehyde-benzyl alcohol interconversion:



where X = H- or CH₃O-.

Solvent isotope effects were investigated to determine the extent to which proton transfer is kinetically coupled to hy-

[†] From the Department of Chemistry, University of California, Berkeley, California 94720. Received October 31, 1979. This work was initiated at the Institute for Cancer Research, Philadelphia, PA, and was supported by National Institutes of Health Grant 5 RO1 GM25765. Preliminary accounts of this work appeared in Klinman (1978a) and Klinman et al. (1977).

[‡] Present address: Department of Biochemistry and Biophysics, University of Pennsylvania, Philadelphia, PA 19174.

[§] Present address: Department of Chemistry, University of Maryland, Baltimore County, Cantonsville, MD 21228.

drogen transfer between coenzyme and substrate. Secondary isotope effects are powerful probes of transition-state structure and were undertaken as a measure of bond hybridization changes at C-1 of substrate in the transition state. Several critical findings from these studies are (1) proton transfer is uncoupled from C-H cleavage and (2) the transition state resembles aldehyde with regard to bond hybridization at C-1, in marked contrast to previously reported structure-reactivity correlations which indicate a charge distribution at C-1 resembling that of alcohol (Klinman, 1976). The implications of these findings to the alcohol dehydrogenase mechanism are discussed.

Experimental Section

Commercial chemicals were reagent grade or better unless specified. Benzaldehyde (Fisher) and *p*-methoxybenzaldehyde (Eastman) were vacuum-distilled prior to use (*p*-CH₃O, bp 83 °C at 2 mmHg; *p*-H, bp 62 °C at 10 mmHg). Tetrahydrofuran (Aldrich, 99.5+%) was distilled from LiAlH₄ (bp 66 °C), acetonitrile (Matheson Coleman and Bell) was distilled from NaH (bp 82 °C), and diethyl ether was distilled (Baker) from P₂O₅ (bp 35 °C). Methylene chloride (Fisher) was washed with 5% Na₂CO₃, H₂O, and saturated NaCl, dried over anhydrous CaCl₂, and distilled (bp 40 °C). Both 1,3-propanedithiol and *n*-butyllithium (1.6 M solution in hexane) were supplied by Aldrich and used without further purification. Deuterium oxide (Wilmad; 99.8% D) was purified by bulb to bulb distillation prior to use. Semicarbazide hydrochloride (99+%) was from Aldrich, sodium pyruvate was from Sigma Chemical Co., acetylpyridine adenine dinucleotide was from Boehringer Mannheim, and NAD⁺ (alcohol free) and NADH were from P-L Biochemicals. Ammonium sulfate, ultrapure grade, was from Schwarz/Mann. Technical-grade hydrogen chloride gas was from Matheson Gas Products, and ceric ammonium nitrate was from G. Frederick Smith. New England Nuclear was the source of radioactive materials: tritiated water (1 Ci/g) and sodium borohydride (100 mCi/mmol). Yeast alcohol dehydrogenase and rabbit muscle lactate dehydrogenase were obtained as ammonium sulfate suspensions from Boehringer Mannheim; horse liver alcohol dehydrogenase and yeast aldehyde dehydrogenase were from Worthington and Boehringer Mannheim, respectively.

Two types of precoated silica gel thin-layer plates were used. Preparative Sil G-25 plates were from Macherey-Nagel Co. (10 × 25 cm; 0.25 mm thick). For analysis of experimental reactions, silica gel 60 with fluorescent indicator F-254 (5 × 10 cm; 0.25 mm thick) from EM Laboratories was utilized.

Radioactivity was determined on an Intertechnique scintillation spectrometer with a PPO-POPOP-toluene-ethanol cocktail. 1,4-Bis[2-(4-methyl-5-phenyloxazolyl)]benzene (dimethyl-POPOP) was from Packard (scintillation grade) and 2,5-diphenyloxazole (PPO) was from New England Nuclear (scintillation grade). A Radiometer (type TTT1C) pH meter was used for pH determinations. All absorbance spectroscopic determinations were carried out on a Cary 118B. Nuclear magnetic resonance spectra were determined on a Varian HA-100.

Copurification of Benzyl Alcohol and Benzaldehyde Dehydrogenase. *Pseudomonas* cells were aerobically cultured in 12-gal glass bottles containing media as described by Suhara et al. (1969), with the exception that freshly distilled benzyl alcohol at 0.1% by volume was used as the sole carbon source. The cells were collected by continuous centrifugation with a Sorvall Svent-Gyorgyi and Blum continuous flow system in a Sorvall RC-2 centrifuge at 8300g. The pelleted cells were resuspended in 0.9% NaCl and centrifuged at 8300g for 30

min, and the pellet was stored frozen.

The two enzymatic activities were copurified by a modification of the procedure of Katagiri et al. (1967). Frozen *Pseudomonas* cells (106 g) were suspended in acetone buffer (50 mM KP_i at pH 7.5, 10% acetone, and 0.1 mM dithiothreitol) containing 1 mM EDTA. When completely thawed, the cell suspension was lysed in a French pressure cell manufactured by the American Instrument Co. This required two passes of the suspension at a pressure of 15000 psi. The resultant lysate was centrifuged at 8300g for 30 min. The pH of the supernatant was titrated to 6.5 with 2 N NH₄OH. A 2% protamine sulfate solution was added to the supernatant to obtain a final concentration of 0.33%. Centrifugation at 10900g for 30 min yielded a supernatant which was raised in pH to 7.5 with 2 N NH₄OH. This was followed by precipitation with ammonium sulfate at both 40 and 55% saturation. Throughout the ammonium sulfate fractionation, the pH was maintained at 7.5 with 2 N NH₄OH. The desired enzymatic activities were precipitated at 55% ammonium sulfate and were redissolved in acetone buffer.

The dissolved 55% ammonium sulfate precipitate was dialyzed against acetone buffer prior to application on a DE-52 column (2.5 × 58 cm) equilibrated with 50 mM KP_i, pH 7.5, and 10% acetone. The column was eluted with a linear gradient of ammonium sulfate achieved with 300 mL of acetone buffer in the mixing chamber and 300 mL of acetone buffer containing 15 g of ammonium sulfate in the reservoir. The two enzymatic activities eluted in the same region of the gradient with the aldehyde dehydrogenase activity appearing primarily in the front portion of the alcohol dehydrogenase activity. The two activities were pooled together and concentrated by precipitation with ammonium sulfate at 40 and 55%. The 55% precipitate was dissolved in acetone buffer and dialyzed against the same buffer prior to being divided into small aliquots and stored frozen at -70 °C.

The entire purification was done at 4 °C. The final yield of protein was 160 mg representing 3400 units of alcohol dehydrogenase activity and 1300 units of aldehyde dehydrogenase activity. Alcohol dehydrogenase activity was assayed in 40 mM KPP_i, pH 8.5, 9 mM benzyl alcohol, and 0.5 mM NAD⁺. Aldehyde dehydrogenase activity was assayed in 40 mM KPP_i, pH 8.5, 4.5 mM benzaldehyde, and 1 mM NAD⁺. In both cases the assay was initiated by the addition of enzyme. It should be noted that the substrate extinction coefficient for aldehyde dehydrogenase was 6.22 cm⁻¹ mM⁻¹ while the apparent extinction coefficient for alcohol dehydrogenase was 12.44 cm⁻¹ mM⁻¹, due to the production of 2 mol of NADH for each mol of alcohol completely oxidized to acid. Protein concentration was determined by the method of Lowry (1951).

Synthesis of [1-³H]Benzaldehyde and [1(S)-³H]Benzyl Alcohol. 2-Phenyl-1,3-dithiane was synthesized according to the procedure of Seebach et al. (1966). Hydrogen chloride gas was bubbled rapidly for 5 min into a solution of 300 mL of CHCl₃ containing 0.41 mol of both 1,3-propanedithiol and freshly distilled benzaldehyde. After an additional 0.5 h, the CHCl₃ phase was washed twice with water, 10% KOH, and water and then filtered through anhydrous sodium sulfate. Chloroform was removed by flash evaporation, and the resultant residue was dissolved in hot methanol, filtered through charcoal, and crystallized from methanol in 74% overall yield.

The hydrogen on C-2 of the dithiane was exchanged with tritium to generate the desired radiolabeled 2-phenyl-1,3-dithiane. The exchange was achieved by a modification of the procedure of Seebach et al. (1966). The above dithiane (4.7

mmol) was dissolved in 8.8 mL of freshly distilled, dry tetrahydrofuran. The reaction was kept under nitrogen and the temperature was lowered to that of a dry ice-acetone bath. Over a 1-h period *n*-butyllithium (4.4 mmol) was added. Tritiated acetic acid (4.4 mmol equiv of tritium) was added and the solution was allowed to come to room temperature overnight. The tritiated acetic acid had been generated by incubating 1.9 mmol of acetic anhydride with 2.22 mmol of tritiated H₂O (sp act. 8×10^6 cpm/ μ mol) in a sealed glass tube at 90 °C for 1 h, followed by bulb to bulb distillation under vacuum immediately prior to addition to the reaction flask.

After being allowed to stand overnight, 0.5 mL of 50 mM hydrochloric acid was added to the reaction flask, and the tetrahydrofuran was removed by distillation under vacuum. The residue was dissolved in CHCl₃ and washed with 10% NaHCO₃, H₂O, and saturated NaCl. The CHCl₃ phase was then dried with anhydrous Na₂CO₃, and the CHCl₃ was removed under nitrogen. Product was crystallized from methanol and stored frozen.

Tritiated benzaldehyde was generated according to a modification of the procedure of Ho et al. (1972) for dethioacetalization with ceric ammonium nitrate. Tritiated dithiane (102 μ mol; sp act. 1.23×10^6 cpm/ μ mol) was dissolved in 1.25 mL of 4:1 acetonitrile-H₂O. Ceric ammonium nitrate (541 μ mol) was added and mixed vigorously for 3 min at which time 1.3 mL of an ice-H₂O mix was added. This solution was extracted twice with 1 mL of ether, and the combined ether phases were washed twice with 0.4 mL of 10% KOH and dried over anhydrous Na₂SO₄. The ether was evaporated under nitrogen, and the resultant benzaldehyde was dissolved in H₂O, bulb to bulb distilled, and stored frozen. Typical yields were 30–40% with a specific activity of 1.26×10^6 cpm/ μ mol.

Isotopically labeled benzyl alcohol was prepared enzymatically from the above benzaldehyde. [1-³H]Benzaldehyde (40 μ mol) and NADH (70 μ mol) were incubated in 80 mM KP_i (pH 6.8) in the presence of 0.7 unit of liver alcohol dehydrogenase. After 1.5 h, the reaction was extracted into CH₂Cl₂. The organic phase was concentrated under nitrogen and applied to thin-layer silica gel plates which were developed in a solvent system of 19:1 CH₂Cl₂-ether. The alcohol was located by radioactivity, the appropriate section was scraped from the plate, and the gel was eluted with ether. The ether was removed under nitrogen, and the resultant alcohol was dissolved in H₂O and distilled bulb to bulb under vacuum and stored frozen. The resulting benzyl alcohol solution was 47 mM, specific activity 1.35×10^6 cpm/ μ mol.

Synthesis of p-Methoxy[1-³H]benzaldehyde and p-Methoxy[1(S)-³H]benzyl Alcohol. All syntheses were similar to those described above, with the following variations. 2-(4-Methoxyphenyl)-1,3-dithiane was synthesized from freshly distilled *p*-methoxybenzaldehyde (0.164 mol). The resultant dithiane was crystallized from 2:1 methanol-CHCl₃ in a yield of 85%. The hydrogen at C-2 of the dithiane was exchanged for tritium as described above except that crystallization again required 2:1 methanol-CHCl₃. The specific activity of the resultant tritiated dithiane was 4.0×10^5 cpm/ μ mol. Synthesis of the aldehyde required a 6:1 acetonitrile-H₂O mixture to achieve solubilization but otherwise was identical with the above. The yield of aldehyde was 40% with a specific activity of 4.2×10^5 cpm/ μ mol. *p*-Methoxybenzyl alcohol was synthesized exactly as described for benzyl alcohol. The resulting alcohol solution was 20 mM, specific activity 4.0×10^5 cpm/ μ mol.

Synthesis of [1(R)-³H]Benzyl Alcohol. *Pro-R* tritiated benzyl alcohol was generated indirectly from tritiated sodium borohydride, prepared by adding 25 mCi of [³H]NaBH₄ to 0.39 mmol of unlabeled NaBH₄ dissolved in 0.15 N NaOH for a total of 0.50 mmol, specific activity 1×10^8 cpm/ μ mol. The [³H]NaBH₄ was mixed with 2 mmol of freshly distilled acetaldehyde and allowed to react for 10 min, followed by an additional 78 μ mol of unlabeled NaBH₄ for 5 min. The reaction was stopped by dropping the pH below 7 with 5 N HCl. Tritiated ethanol (1.3 mmol) was recovered by bulb to bulb distillation, specific activity 3.5×10^6 cpm/ μ mol.

Stereospecifically tritiated NADH was synthesized enzymatically from the above ethanol by using yeast alcohol and aldehyde dehydrogenases. The reaction was carried out in 500 mM Tris (pH 9) containing 2.6 mmol of NAD⁺, 1.3 mmol of tritiated ethanol, 30 mg of yeast alcohol dehydrogenase, and 16 mg of yeast aldehyde dehydrogenase, yielding a mixture of reduced and oxidized coenzymes together with acetaldehyde, acetic acid, and ethanol. When no further optical density change at 340 nm could be detected (corresponding to 50% conversion), the reaction mixture was heated to denature the enzymes. The solution was diluted 10-fold and NADH was prepared according to the procedure of Rafter & Colowick (1957). The yield of coenzymes was 2.3 g of which 57% represented NADH, specific activity 1.45×10^6 cpm/ μ mol.

Finally, [1(R)-³H]benzyl alcohol was synthesized enzymatically from 26 μ mol of [4(R)-³H]NADH and 30 μ mol of benzaldehyde in 80 mM KP_i (pH 6.8) containing 0.7 unit of LADH. After 90% of the absorbance due to NADH was lost, the reaction was quenched by extraction with CH₂Cl₂. The CH₂Cl₂ phase was concentrated under nitrogen and applied to a preparative silica gel thin-layer plate, which was developed with 19:1 CH₂Cl₂-ether. Alcohol was located by radioactivity, the appropriate area was scraped from the plate, and the gel was eluted twice with 5 mL of ether. The combined ether phase was evaporated under N₂, and the remaining alcohol was dissolved in water, distilled bulb to bulb under vacuum, and stored frozen. The benzyl alcohol solution was 33 mM, specific activity 6.6×10^5 cpm/ μ mol.

Synthesis of [4(R)-²H]NADH. [4(R)-²H]NADH was prepared enzymatically from NAD⁺ according to the method of Rafter & Colowick (1957) employing ethyl alcohol-*d*₅, 98 atom % deuterium (Merck Sharp and Dohme of Canada). The isotopic purity of product was confirmed by nuclear magnetic resonance. We had previously shown that NADH synthesized in parallel with [4(R)-²H]NADH is characterized by the same kinetic properties as commercial NADH; hence, the present studies were carried out with NADH from P-L Biochemicals. Solutions of the sodium salt of NADH and [4(R)-²H]NADH were prepared and assayed as described (Klinman, 1972).

Measurement of Solvent Isotope Effects. Yeast alcohol dehydrogenase was extensively dialyzed prior to use. *p*-Methoxybenzyl alcohol and *p*-methoxybenzaldehyde were vacuum distilled and used immediately for kinetic studies; solutions of coenzymes and substrates were assayed enzymatically (Klinman, 1972, 1976). Kinetic measurements were carried out at 25 °C, $\mu = 0.22$, by following the appearance or disappearance of NADH at 340 nm. Intercepts from primary Lineweaver-Burk plots were replotted as a function of second substrate to obtain V_{max} ; rate constants were calculated from V_{max} assuming four active sites per mol of enzyme and normalized to a specific activity of 100 units/mg (Klinman, 1972, 1976). KP_i and KPP_i-glycine buffers were employed in the pH range 7.2–9.2. Buffer and coenzyme solu-

tions were prepared in H₂O and lyophilized to dryness and redissolved 2 times in H₂O or D₂O. pD = pH(meter) + 0.4. The final concentration of H₂O in lyophilized D₂O reaction mixtures was determined by nuclear magnetic resonance using tetramethylsilane as an external standard.

Measurement of Kinetic α -Secondary Isotope Effects in the Direction of Alcohol Oxidation. Both a chemical and an enzymatic coupling system were used to pull the reaction against an unfavorable equilibrium. Chemically, 8 mM benzyl alcohol (4 mM for *p*-methoxybenzyl alcohol) and 20 mM NAD⁺ (11 mM for *p*-methoxybenzyl alcohol) were coupled with 100 mM semicarbazide. The reactions were run at pH 9.0, 80 mM PP_i. Yeast alcohol dehydrogenase (0.8–1.6 mg/mL) was added to initiate the reaction. The progress of the reaction was monitored at 340 nm for the formation of NADH.

Enzymatically, lactate dehydrogenase at 0.3–6 times the molar concentration of yeast alcohol dehydrogenases was used in the presence of 10 mM pyruvate to recycle the NADH. To 8 mM benzyl alcohol (8 mM *p*-methoxybenzyl alcohol) and 10 mM NAD⁺ (2.6 mM for *p*-methoxybenzyl alcohol) in 40 mM PP_i, pH 8.5, were added lactate and yeast alcohol dehydrogenases to initiate the reaction. The course of the reaction was followed by monitoring the depletion of pyruvate. Pyruvate concentrations were determined from the change in optical density at 340 nm following the addition of 10 μ L of reaction mixture to a cuvette containing 0.1 M P_i, pH 7.0, 0.39 mM NADH, and 1.8 units of lactate dehydrogenase.

At varying times in the course of the reaction, aliquots of the reaction mixture were extracted twice with an equal volume of CH₂Cl₂. The CH₂Cl₂ phase was concentrated and applied to thin-layer silica gel chromatography plates and developed with 19:1 CH₂Cl₂-ether. The benzyl alcohols were located by fluorescence, scraped from the plate, and eluted twice with H₂O. Alcohol concentration was assayed by using alcohol and aldehyde dehydrogenase isolated from pseudomonas cells with a net extinction coefficient of 12.44 cm⁻¹ mM⁻¹ at 340 nm.

Measurement of Kinetic α -Secondary Isotope Effects in the Direction of Aldehyde Reduction. To 8 mM benzaldehyde (4 mM for *p*-methoxybenzaldehyde) in the presence of 15 mM NADH (6.2 mM for *p*-methoxybenzaldehyde) and 40 mM PP_i, pH 8.5 (80 mM P_i, pH 7.3, for *p*-methoxybenzaldehyde), was added yeast alcohol dehydrogenase (0.15–0.5 mg/mL) to initiate the reaction. The reaction course was determined by assaying for unreacted aldehyde. Aliquots of the reaction were removed at varying times and treated as described above for alcohol oxidation.

Measurement of Equilibrium α -Secondary Isotope Effects. Equilibrium isotope effects were determined under a variety of conditions as defined in Table VI. In all cases the reactions were initiated with enzyme and followed spectrophotometrically at 340 nm. The specific activity of alcohol was determined following extraction of the reaction mixtures with CH₂Cl₂, followed by purification of alcohol on silica gel thin-layer plates as described above for alcohol oxidation.

Results

Previous studies of the effect of pH on steady-state kinetic parameters for the yeast alcohol dehydrogenase catalyzed reduction of acetaldehyde vs. oxidation of *p*-methoxybenzyl alcohol indicated crossing titration curves of the same pK_a (\approx 8.25) (Klinman, 1975), consistent with a dependence on different enzyme forms for aldehyde reduction (the protonated form of an enzyme functional group, E–BH) vs. alcohol oxidation (the free base form of an enzyme functional group, E–B). In order to distinguish solvent isotope effects on rate

Table I: Solvent Isotope Effects on k_{obsd} for Reduction of *p*-Methoxybenzaldehyde by NADH, Catalyzed by Yeast Alcohol Dehydrogenase

pL ^a	$k_{\text{H}_2\text{O}}^b$ (s ⁻¹)	$k_{\text{D}_2\text{O}}^b$ (s ⁻¹)	$k_{\text{D}_2\text{O}}/k_{\text{H}_2\text{O}}$
pH 7.19 pD 7.20	0.141 ± 0.009	0.271 ± 0.026	1.92 ± 0.33
pH 7.58 pD 7.61	0.127 ± 0.004	0.196 ± 0.012	1.54 ± 0.15
pH 8.09 pD 8.15	0.100 ± 0.01	0.145 ± 0.016	1.45 ± 0.34
pH 8.59 pD 8.65	0.072 ± 0.011	0.145 ± 0.016	2.01 ± 0.60

^a pL is a general term referring to pH (in H₂O) and pD (in D₂O).
^b $k_{\text{H}_2\text{O}}$ and $k_{\text{D}_2\text{O}}$ were determined from the intercepts of replots of intercepts, obtained by extrapolation of Lineweaver–Burk plots to infinite concentrations of NADH and aldehyde, as a function of aldehyde and NADH concentrations, respectively.

Table II: Solvent Isotope Effects on k_{obsd} for the Reduction of *p*-Methoxybenzaldehyde by [4(*R*)-²H]NADH, Catalyzed by Yeast Alcohol Dehydrogenase

pL ^a	$k_{\text{H}_2\text{O}}^b$ (s ⁻¹)	$k_{\text{D}_2\text{O}}^b$ (s ⁻¹)	$k_{\text{D}_2\text{O}}/k_{\text{H}_2\text{O}}$
pH 7.17 pD 7.18	0.0485 ± 0.0039	0.0773 ± 0.0095	1.59 ± 0.36
pH 7.58 pD 7.61	0.0339 ± 0.0010	0.0715	2.11 ± 0.05
pH 8.09 pD 8.15	0.0281 ± 0.0021	0.0476 ± 0.0019	1.69 ± 0.21
pH 8.59 pD 8.65	0.0260 ± 0.002	0.040	1.54 ± 0.11

^a pL is a general term referring to pH (in H₂O) and pD (in D₂O).
^b $k_{\text{H}_2\text{O}}$ and $k_{\text{D}_2\text{O}}$ were determined from the intercepts of replots of intercepts, obtained by extrapolation of Lineweaver–Burk plots to infinite concentrations of [4-²H]NADH and aldehyde, as a function of aldehyde and [4-²H]NADH concentrations, respectively.

Table III: Solvent Isotope Effects on k_{obsd} for *p*-Methoxybenzyl Alcohol Oxidation by NAD⁺, Catalyzed by Yeast Alcohol Dehydrogenase

pL ^a	$k_{\text{H}_2\text{O}}^b$ (s ⁻¹)	$k_{\text{D}_2\text{O}}^b$ (s ⁻¹)	$k_{\text{H}_2\text{O}}/k_{\text{D}_2\text{O}}$
pH 7.61 pD 7.63	0.170 ± 0.015	0.103 ± 0.006	1.65 ± 0.20
pH 7.83 pD 7.91	0.189 ± 0.013	0.142	1.33 ± 0.09
pH 8.11 pD 8.13	0.399 ± 0.061	0.212 ± 0.014	1.88 ± 0.44
pH 8.62 pD 8.62	0.416 ± 0.066	0.448 ± 0.014	0.93 ± 0.18
pH 9.17 pD 9.24	0.776 ± 0.021	0.648 ± 0.030	1.20 ± 0.09

^a pL is a general term referring to either pH (in H₂O) or pD (in D₂O).
^b $k_{\text{H}_2\text{O}}$ and $k_{\text{D}_2\text{O}}$ were determined from the intercepts of replots of intercepts, obtained by extrapolation of Lineweaver–Burk plots to infinite concentrations of both NAD⁺ and alcohol, as a function of alcohol and NAD⁺ concentrations, respectively.

from pK_a, the effect of D₂O on rate constants, obtained from the extrapolation of Lineweaver–Burk plots to infinite concentration of substrate and coenzyme for the *p*-methoxybenzaldehyde/*p*-methoxybenzyl alcohol interconversion, was investigated in the pH range 7.2–9.2 (Tables I and III). Solvent isotope effects were also measured for *p*-methoxybenzaldehyde reduction by [4(*R*)-²H]NADH, in an effort to demonstrate that a decrease in the rate of hydrogen transfer

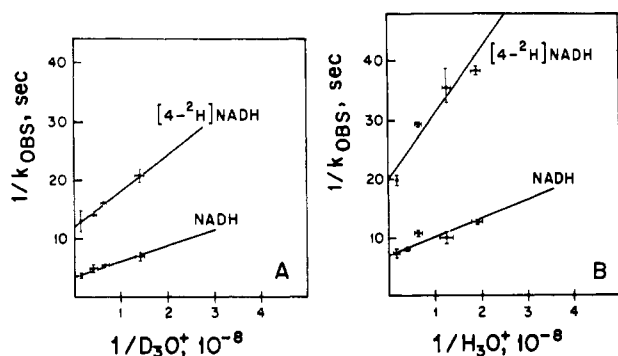


FIGURE 1: (A) Reduction of *p*-methoxybenzaldehyde by NADH and [4-²H]NADH in D₂O. Values of k_{obsd} (obtained by extrapolation to infinite substrate and coenzyme concentrations) at a given pH have been plotted according to eq 3. (B) Reduction of *p*-methoxybenzaldehyde by NADH and [4-²H]NADH in H₂O. Values of k_{obsd} (obtained by extrapolation to infinite substrate and coenzyme concentrations) at a given pH have been plotted according to eq 3.

Table IV: Solvent Isotope Effects on pK_a^a

substrate	pK_a		
	H ₂ O	D ₂ O	ΔpK_a
<i>p</i> -methoxybenzaldehyde reduction	8.27	8.29	0.02
<i>p</i> -methoxybenzyl alcohol oxidation	8.14	8.35	0.21

^a Obtained from slopes and intercepts of Figures 1 and 2, as described in the text, eq 2-5.

from coenzyme to substrate by a factor of 3-5 (Klinman, 1972) leads to an unaltered solvent isotope effect (Table II).

The analysis of the data in Tables I-III is facilitated by reciprocal plots of the observed rate constants at a given pH as a function of the hydronium ion activity. On the assumption that catalysis of aldehyde reduction can only occur from the protonated form of enzyme, one obtains

$$V = k_{\text{cat}}[E-BH] = \frac{k_{\text{cat}}[E_T]}{1 + K_a/[H_3O^+]} \quad (2)$$

Restatement of eq 2 in reciprocal form leads to

$$\frac{[E_T]}{V} = \frac{1}{k_{\text{obsd}}} = \frac{1}{k_{\text{cat}}} + \frac{K_a}{k_{\text{cat}}[H_3O^+]} \quad (3)$$

Plots of $1/k_{\text{obsd}}$ vs. $1/[D_3O^+]$ or $1/[H_3O^+]$ are illustrated in parts A and B of Figure 1 for *p*-methoxybenzaldehyde reduction by NADH and [4(*R*)-²H]NADH in D₂O and H₂O, respectively. The intercepts of these plots provide k_{cat} [where $E-BH(D) = E_T$], and the negative log of the ratio of slopes to intercepts gives pK_a . The major findings, summarized in Tables IV and V, are (1) an unusually small effect of D₂O in the pK_a of the ionizing residue (Table IV) and (2) an *inverse* solvent isotope effect on k_{cat} which is essentially unchanged for reduction by [4-²H]NADH vs. NADH (Table V).

Table V: Solvent Isotope Effects on k_{cat}^a

substrate	k_{cat} (s ⁻¹)		k_{H_2O}/k_{D_2O}
	H ₂ O	D ₂ O	
<i>p</i> -methoxybenzaldehyde reduction plus NADH	0.14 ± 0.007	0.28 ± 0.014	0.50 ± 0.05
plus [4- ² H]NADH	0.049 ± 0.002	0.085 ± 0.005	0.58 ± 0.06
<i>p</i> -methoxybenzyl alcohol oxidation	0.78 ± 0.02	0.65 ± 0.03	1.20 ± 0.09

^a Obtained from intercepts in Figures 1 and 2, as described in the text, eq 2-5.

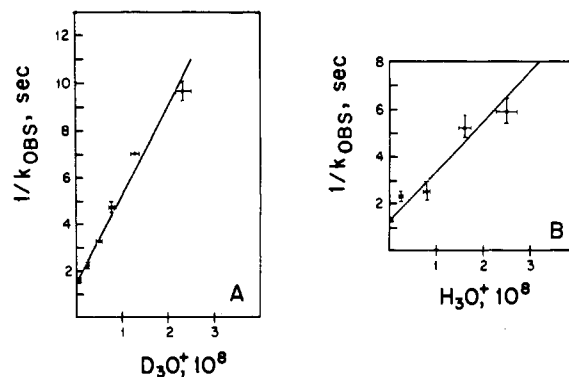


FIGURE 2: (A) Oxidation of *p*-methoxybenzyl alcohol by NAD⁺ in D₂O. Values of k_{obsd} (obtained by extrapolation to infinite substrate and coenzyme concentrations) at a given pH have been plotted according to eq 5. (B) Oxidation of *p*-methoxybenzyl alcohol by NAD⁺ in H₂O. Values of k_{obsd} (obtained by extrapolation to infinite substrate and coenzyme concentrations) at a given pH have been plotted according to eq 5.

A similar analysis of the data in Table III for *p*-methoxybenzyl alcohol oxidation can be carried out, on the assumption that catalysis requires the free base form of enzyme:

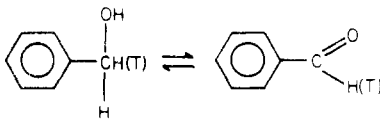
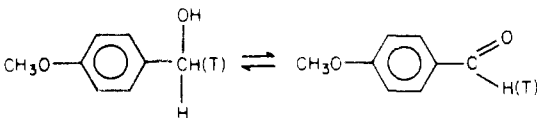
$$V = k_{\text{cat}}[E-B] = \frac{k_{\text{cat}}[E_T]}{1 + [H_3O^+]/K_a} \quad (4)$$

$$\frac{[E_T]}{V} = \frac{1}{k_{\text{obsd}}} = \frac{1}{k_{\text{cat}}} + \frac{[H_3O^+]}{k_{\text{cat}}K_a} \quad (5)$$

Plots of $1/k_{\text{obsd}}$ vs. D_3O^+ and H_3O^+ are illustrated in parts A and B of Figure 2 for *p*-methoxybenzyl alcohol oxidation in D₂O and H₂O, respectively. The intercepts of these plots provide the limiting rate constant (where $E-B = E_T$); from the log of the ratio of the slopes to intercepts, one obtains pK_a for the ionizing residue. Although the ΔpK_a deduced from alcohol oxidation is larger than the value for aldehyde reduction (Table IV), it is still considerably smaller than the common observation of a $\Delta pK_a = 0.4-0.6$. The solvent isotope effect on k_{cat} is not significantly different from 1 (Table V); this result effectively rules out a mechanism in which proton transfer to an active-site base is kinetically coupled to hydrogen transfer from substrate to coenzyme.

α -Secondary Tritium Isotope Effects. Tritium, rather than deuterium, α -secondary isotope effects were measured due to their greater magnitude and independence of potential inhibitory contaminants in isotopically labeled substrates. A single method, involving the purification and specific activity determination of either benzyl alcohol or *p*-methoxybenzyl alcohol, was employed. Both horse liver and yeast alcohol dehydrogenases proved inadequate for the determination of alcohol concentration, due to a low level but persistent contamination of solvents and thin-layer chromatographic plates by ethanol. An assay system was developed, which involves the use of benzyl alcohol and benzaldehyde dehydrogenase to

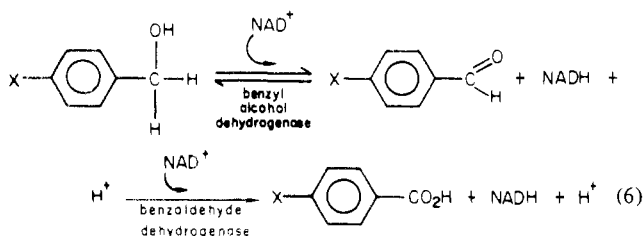
Table VI. Equilibrium α -Secondary Tritium Isotope Effects for the Interconversion of [$1\text{-}^3\text{H}$] Benzaldehydes and [$1(S)\text{-}^3\text{H}$] Benzyl Alcohols, Catalyzed by Yeast Alcohol Dehydrogenase

reaction conditions	sp act. of alcohol at $t_0 \times 10^{-6}$ (cpm/ μmol)	% conversion of alcohol to aldehyde at equilibrium	sp act. of alcohol at equilibrium $\times 10^{-6}$ (cpm/ μmol)	K_H/K_T^b	
 NAD ⁺ (pH 9) ^c acetylpyridine-NAD ⁺ (pH 8.5) ^d	1.46 \pm 0 (2) ^a	17	1.52 \pm 0.05 (3)	1.30	
	1.40 \pm 0.06 (4)	40	1.58 \pm 0.02 (3)	1.40	
	1.45 \pm 0.03 (4)	41	1.61 \pm 0.02 (2)	1.32	
	1.35 \pm 0.04 (4)	76	1.64 \pm 0.09 (6)	1.30	
	mean =				1.33 \pm 0.05
 acetylpyridine-NAD ⁺ (pH 8.5) ^e	0.509 \pm 0.020 (4)	70	0.635 \pm 0.007	1.40	
	0.444 \pm 0.009 (4)	87	0.543 \pm 0.010	1.27	
	mean =				1.34 \pm 0.09

^a Specific activities reported as mean \pm standard deviation; values in parentheses represent the number of independent determinations.

^b Where K_T/K_H = specific activity of alcohol/specific activity of aldehyde. Specific activity of aldehyde was calculated from the following relationship: specific activity of alcohol (at t_0) = specific activity of alcohol (at equilibrium) \times fraction of alcohol remaining + specific activity of aldehyde (at equilibrium) \times fraction of alcohol converted. ^c The reaction mixture contained 80 mM KPP_i (pH 9.0), 6.4 mM [$1(S)\text{-}^3\text{H}$] benzyl alcohol, 12.3 mM NAD⁺, and 463 units of yeast alcohol dehydrogenase. ^d The reaction mixture contained 40 mM KPP_i (pH 8.5), 2.3 mM [$1(S)\text{-}^3\text{H}$] benzyl alcohol, 1.8–11 mM acetylpyridine-NAD⁺, and 0.05–0.1 unit of horse liver alcohol dehydrogenase. ^e The reaction mixture contained 40 mM KPP_i (pH 8.5), 1.1–1.6 mM *p*-methoxy[$1(S)\text{-}^3\text{H}$] benzyl alcohol, 1.1–2.5 mM acetylpyridine-NAD⁺, and 0.07 unit of horse liver alcohol dehydrogenase.

assay for benzyl alcohols. The value of this coupled assay is (1) its specificity for aromatic alcohols, (2) its irreversibility, and (3) its sensitivity, since 2 mol of NADH are produced per mol of alcohol oxidized:



Equilibrium α -secondary isotope effects provide the frame of reference for the interpretation of kinetic isotope effects. These measurements are preferably carried out with acetylpyridine-NAD⁺, since this coenzyme leads to a greater percent conversion of alcohol to aldehyde at equilibrium [acetylpyridine-NAD⁺ favors aldehyde production by 2 orders of magnitude relative to NAD⁺ (Racker, 1950; Holzer & Söling, 1962)]. The values (Table VI) indicate no difference, within experimental error, between unsubstituted and para-substituted substrate; the observed magnitude of K_H/K_T is consistent with a range of previously reported values for analogous $\text{sp}^3 \rightleftharpoons \text{sp}^2$ interconversions at carbon (Klinman, 1978b).

Kinetic isotope effects in the direction of aldehyde reduction are summarized in Table VII. For benzaldehyde reduction, a comparison of specific activities for product alcohol at early percent conversion to the specific activity of alcohol at infinity indicated little or no isotope effect, $k_H/k_T = 1.02 \pm 0.03$. Longer time points were taken in the case of *p*-methoxybenzaldehyde reduction, demonstrating both the absence of

a significant kinetic isotope effect and the insensitivity of this effect to percent conversion.

Our failure to detect a kinetic α -secondary isotope effect for aldehyde reduction, indicating little or no change in bond hybridization at C-1 of substrate in the transition state, was unexpected. Both benzaldehyde and *p*-methoxybenzaldehyde are essentially unhydrated in solution and the absence of an isotope effect cannot be attributed to a cancellation of an equilibrium isotope effect on a dehydration equilibrium by a kinetic isotope effect for carbonyl reduction.

The measurement of α -secondary kinetic isotopes in the direction of alcohol oxidation was undertaken, in an effort to corroborate the results for aldehyde reduction. Accurate measurements of isotope effects in the direction of alcohol oxidation required pulling the reaction against an unfavorable equilibrium; this was achieved either chemically, by trapping product benzaldehyde with semicarbazide, or enzymatically, by recycling product NADH to NAD⁺ with pyruvate and lactate dehydrogenase. The latter method led to more accurate isotope effects for both benzyl alcohol (Table VIII) and *p*-methoxybenzyl alcohol oxidation (Table IX). Importantly, the quotient of kinetic isotope effects for alcohol oxidation and aldehyde reduction is within experimental error of the equilibrium isotope effect, ruling out experimental artifact as the source of the unusually small kinetic isotope effect in the direction of aldehyde reduction.

In light of the similarity of the magnitudes of k_H/k_T for alcohol oxidation to K_H/K_T , an additional control was carried out to establish that hydrogen transfer from alcohol to coenzyme was limiting V_{max}/K_m under the experimental conditions of our secondary isotope effect measurements. Previously reported deuterium isotope effects on V_{max}/K_m were

Table VII: Kinetic α -Secondary Tritium Isotope Effects for Reduction of [1- ^3H] Benzaldehydes by NADH, Catalyzed by Yeast Alcohol Dehydrogenase

% conversion	sp act. ^a of alcohol $\times 10^{-6}$ (cpm/ μmol)	$k_{\text{H}}/k_{\text{T}}^{\text{b}}$
6.1	1.37 ± 0.01 (2) ^a	1.01
10	1.30 ± 0.03 (4)	1.06
11	1.39 ± 0.04 (4)	0.99
12	1.34 ± 0.02 (4)	1.03
13	1.35 ± 0.07 (3)	1.02
∞	1.38 ± 0.06 (23)	
	mean: 1.02 ± 0.03	
9.8	0.453 ± 0.001 (2)	1.04
22.5	0.465 ± 0.006 (2)	1.01
53	0.437 ± 0.009 (2)	1.11
∞	0.470 ± 0.008 (3)	
	mean: 1.05 ± 0.05	

^a Specific activity given as mean \pm standard deviation; values in parentheses represent the number of independent determinations.
^b Where $k_{\text{T}}/k_{\text{H}} = \ln [1 - (\text{fraction of aldehyde converted})] [\text{sp act.} (t)/\text{sp act.} (t_{\infty})] / \ln (\text{fraction of aldehyde remaining})$, as described in Melander (1960).

3.5 and 2.8 for benzaldehyde and *p*-methoxybenzaldehyde reduction, respectively, and 4.3 and 3.5 for benzyl alcohol and *p*-methoxybenzyl alcohol oxidation, respectively. Measurement of the tritium isotope effects for the oxidation of [1(*R*)- ^3H]-benzyl alcohol, employing either semicarbazide or pyruvate and lactate dehydrogenase as trapping reagents, led to a mean value of 5.6 ± 1.1 . The appropriate reference deuterium isotope effect is $(V/K)_{\text{H}}/(V/K)_{\text{D}} = 3.6$ [the observed deuterium isotope effect on $V_{\text{max}}/K_{\text{m}}$ corrected for a secondary isotope effect, since the oxidation of [2(*R*)- $^2\text{H}_2$]-benzyl alcohol had been studied (Klinman, 1976)]. The finding that our measured primary tritium isotope effect is within experimental error of the predicted value employing the Swain-Schaad relationship (Swain et al., 1958), $3.6^{1.44} = 6.3$, indicates that hydrogen transfer from alcohol to NAD^+ is fully rate determining and that our measured secondary tritium isotope effects reflect bond hybridization changes in the chemical transformation step per se.

Discussion

Acid-Base Catalysis. The precise mechanism of acid-base catalysis in the alcohol dehydrogenase reaction has received considerable attention in the literature. Although the available X-ray structure of horse liver alcohol dehydrogenase at 2.4-Å resolution clearly indicates the presence of a ZnOH_2 at the enzyme active site (Eklund et al., 1976), interpretation of the pH dependence of kinetic parameters in terms of a single active-site residue has been complicated by the differential effects of coenzyme and substrate on the pK_a of a critical functional group (Klinman, 1980). In addition, there is a marked asymmetry of the pH dependence for the interconversion of the ternary complex: in the case of aldehyde reduction, k_{cat} is essentially independent of pH in the range of 6.0–9.0 (McFarland & Chu, 1975; Kvassman & Pettersson,

Table VIII: Kinetic α -Secondary Isotope Effect for the Oxidation of [1(*S*)- ^3H] Benzyl Alcohol by NAD^+ , Catalyzed by Yeast Alcohol Dehydrogenase

% conversion	semicarbazide hydrochloride ^a		lactate dehydrogenase ^b	
	sp act. of alcohol $\times 10^{-6}$ (cpm/ μmol)	$k_{\text{H}}/k_{\text{T}}^{\text{d}}$	sp act. of alcohol $\times 10^{-6}$ (cpm/ μmol)	$k_{\text{H}}/k_{\text{T}}^{\text{d}}$
36	1.61 ± 0.01 (2) ^c	1.46		
39	1.61 ± 0.07 (2)	1.39	1.62 ± 0.04 (2)	1.43
47	1.59 ± 0.04 (2)	1.26		
49			1.72 (1)	1.44
50	1.65 ± 0.08 (2)	1.31		
52			1.68 ± 0.04 (4)	1.33
59	1.72 ± 0.08 (2)	1.30		
60	1.60 ± 0.13 (2)	1.17	1.79 ± 0.03 (2)	1.37
63			1.88 ± 0.09 (4)	1.42
65			1.79 ± 0.01 (2)	1.31
70	2.02 ± 0.04 (2)	1.43		
72			1.95 ± 0.08 (2)	1.35
74			1.94 ± 0.01 (2)	1.32
75			1.91 ± 0.10 (6)	1.29
79	1.97 ± 0.37 (2)	1.28		
82			2.12 (1)	1.32
84			1.90 ± 0.07 (2)	1.20
		mean =		mean =
		1.33 \pm		1.34 \pm
		0.10		0.07

^a Semicarbazide added to trap benzaldehyde, as described in detail under Experimental Section. ^b Lactate dehydrogenase added to recycle NADH to NAD^+ , as described in detail under Experimental Section. ^c Specific activity given as mean \pm standard deviation; values in parentheses represent the number of independent determinations. Specific activity (t_0) = 1.40×10^6 ; the standard error and number of determinations varied for each experiment. The standard errors were as follows in the semicarbazide experiment, proceeding down the column: ± 0.06 (4); ± 0.03 (4); ± 0.11 (4); ± 0.03 (4); ± 0.03 (4); ± 0.11 (4); ± 0.03 (4); ± 0.03 (4); ± 0.03 (4); ± 0.03 (4). The standard errors were as follows in the lactate dehydrogenase experiment: ± 0.03 (4); ± 0.03 (4); ± 0.02 (6); ± 0.03 (4); ± 0.02 (6); ± 0.03 (4); ± 0.03 (4); ± 0.03 (4); ± 0.03 (4); ± 0.03 (4). ^d Where $k_{\text{H}}/k_{\text{T}} = \ln (\text{fraction of alcohol remaining}) / \ln [(\text{fraction of alcohol remaining}) [\text{sp act.} (t)/\text{sp act.} (t_0)]]$, as described by Melander (1960).

1978), whereas alcohol oxidation depends on the ionization of a functional group of $\text{pK}_a = 6.4$ (Brooks et al., 1972; Kvassman & Pettersson, 1978). A working model for the horse liver enzyme attributes the range of observed pK_a values (6.4 to >11) to a single active-site residue (ZnOH_2), with the possible exception of the pK_a controlling k_{cat} for alcohol oxidation, which Kvassman & Pettersson (1978) suggest is metal-bound alcohol.

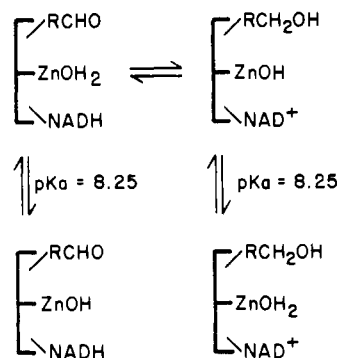
In contrast to horse liver alcohol dehydrogenase, the pH dependence of the interconversion of the ternary complex catalyzed by yeast alcohol dehydrogenase is symmetrical. The available data implicate a single functional group of $\text{pK}_a = 8.25$ which must be protonated for aldehyde reduction and unprotonated for alcohol oxidation (Klinman, 1975). Assignment of this pK_a to ZnOH_2 is somewhat tenuous due to the absence of three-dimensional structural data. Nonetheless, the presence of zinc in the yeast enzyme, the high degree of sequence homology among peptides containing the two cysteine and histidine residues demonstrated to complex the active-site zinc in the horse liver enzyme (Jörnvall et al., 1978), and the similar reactivity of horse liver and yeast enzymes toward a range of active-site-directed alkylating agents (Klinman, 1980) support the presence of ZnOH_2 at the active site of yeast alcohol dehydrogenase (Scheme I).

Scheme I provides a frame of reference for the interpretation of the effects of D_2O on pK_a and k_{cat} (Tables IV and V). The

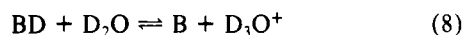
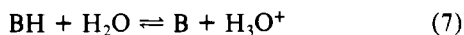
Table IX: Kinetic α -Secondary Isotope Effect for the Oxidation of *p*-Methoxy[1(*S*)-³H]benzyl Alcohol by NAD⁺, Catalyzed by Yeast Alcohol Dehydrogenase

% conversion	semicarbazide hydrochloride ^a		lactate dehydrogenase ^b	
	sp act. of alcohol × 10 ⁻⁵ (cpm/μmol)	k _H /k _T ^d	sp act. of alcohol × 10 ⁻⁵ (cpm/μmol)	k _H /k _T ^d
45	5.53 ± 0.11 (2) ^c	1.41		
57			5.84 ± 0.05 (2)	1.38
64	5.74 ± 0.22 (2)	1.25		
70			6.47 ± 0.18 (2)	1.38
73	6.37 ± 0.24 (2)	1.32		
80			7.10 ± 0.02 (2)	1.36
81	6.86 ± 0.19 (2)	1.31		
89			8.78 ± 0.33 (2)	1.41
		mean = 1.32 ± 0.07		mean = 1.38 ± 0.02

^a Semicarbazide added to trap *p*-methoxybenzaldehyde, as described in detail under Experimental Section. ^b Lactate dehydrogenase added to recycle NADH to NAD⁺, as described in detail under Experimental Section. ^c Specific activity given as mean ± standard deviation; values in parentheses represent the number of independent determinations. Specific activity (*t*₀) = 4.65 × 10⁵; the standard error and number of determinations varied for each experiment. In the semicarbazide experiment the standard error was ±0.18 at each percent conversion. In the lactate dehydrogenase experiment the standard error was ±0.29 at each percent conversion. ^d Where k_H/k_T = ln (fraction of alcohol remaining)/ln [(fraction of alcohol remaining) [sp act. (*t*)/sp act. (*t*₀)]], as described by Melander (1960).

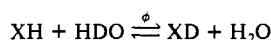
Scheme 1: pK_a Controlling Catalysis in the Yeast Alcohol Dehydrogenase Reaction, Attributed to Ionization of ZnOH₂

effect of D₂O on the kinetically determined pK_a for both aldehyde reduction and alcohol oxidation is considerably less than the common observation of ΔpK_a = pK_D - pK_H = 0.4–0.6. The origin of the effect of D₂O on pK_a is conveniently expressed in terms of fractionation factors φ¹ for the protonic species involved in the equilibria reactions



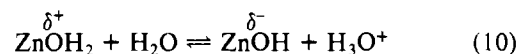
$$pK_D - pK_H = \log \left(\frac{[\text{H}_3\text{O}^+][\text{B}][\text{BD}][\text{D}_2\text{O}]}{[\text{D}_3\text{O}^+][\text{B}][\text{BH}][\text{H}_2\text{O}]} \right) = \log \frac{\phi(\text{BH})}{\phi(\text{H}_3\text{O}^+)} \quad (9)$$

¹ The fractionation factor, φ, describes the isotopic exchange reaction



By definition [H₂O]/[HDO] = 1, and φ simplifies to give [XD]/[XH]. For φ > 1, deuterium will be enriched in XH relative to H₂O.

where [D₂O]/[H₂O] = 1 by definition. For the majority of protonated oxygen and nitrogen bases, φ(BH) = 1 [Schowen (1972, 1978) and references cited therein], and the effect of D₂O on the pK_a of these ionizing residues arises almost exclusively from the fractionation factor for H₃O⁺, φ(H₃O⁺) = 0.33. The small ΔpK_a = 0.02–0.21 observed in the yeast alcohol dehydrogenase system suggests that φ(BH) is similar to φ(H₃O⁺), and on the assumption that BH is monoprotic or that φ(B) = 1, the fractionation factor for BH is calculated to be 0.35–0.54. Thiols are characterized by fractionation factors of ~0.5 (Schowen, 1972, 1978), and two cysteines are known to be present at the active site of yeast alcohol dehydrogenase. However, the above noted homology between horse and yeast alcohol dehydrogenases supports a role for these two cysteines as ligands to an active-site zinc. The fractionation factor for ZnOH₂^{δ+} may not be very different from H₃O⁺ and provides a possible explanation for the small observed effect of D₂O on the pK_a of the active-site residue of yeast alcohol dehydrogenase:

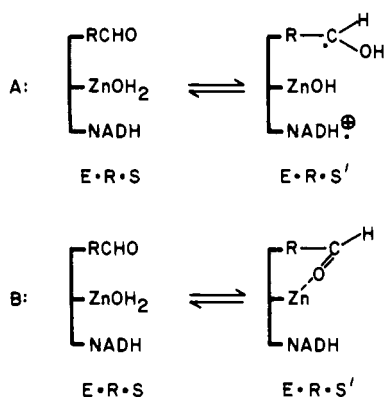


The magnitude of ΔpK_a for the ionization of water complexed to zinc in a well-defined model system has not been reported. Among other metal-bound water complexes, ΔpK_a has been observed to vary from 0.23 for hexaaquoiron(III) (Fukushima & Reynolds, 1964) to 0.48 for aquopentamminecobalt(III) (Splinter et al., 1968); the increase in ΔpK_a is in the same direction as the increase in pK_a from 2.8 to 6.2, analogous to the well-documented relationship between ΔpK_a and pK_a [Laughton & Robertson (1969) and references cited therein]. Thus, the small number of available models suggests that φ(BH) will be close to 1 for the ionization of water in a complex characterized by a pK_a = 8–9, in contrast to the φ(BH) = 0.35–0.54 observed in these studies. Direct examination of the effect of D₂O on the ionization of zinc-bound water would provide valuable data for the interpretation of solvent effects in yeast alcohol dehydrogenase and other zinc-containing enzymes.

The magnitude of solvent isotope effects on *k*_{cat} is summarized in Table V. The kinetic isotope effect can be formulated as the ratio of fractionation factors for the transition state [φ(TS)] and ground state [φ(GS)], k_{H₂O}/k_{D₂O} = φ(GS)/φ(TS). For alcohol oxidation φ(GS) refers to the unprotonated base (ZnOH) and alcoholic hydroxyl group, φ(GS) ≈ 1 and φ(TS) ≈ 1/1.2 = 0.83. In the direction of aldehyde reduction φ(GS) refers to the protonated base (ZnOH₂) and aldehyde carbonyl, φ(GS) ≈ 0.35–0.54 and φ(TS) ≈ (0.35–0.54)/0.50 = 0.70–1.08. A range of studies, which include primary hydrogen isotope effects and structure-reactivity correlations (Klinman, 1972, 1976) and secondary isotope effects (Tables VII–IX), has implicated a single rate-determining C–H bond cleavage step in the yeast alcohol dehydrogenase catalyzed interconversion of aromatic substrates. Consistent with this view, similar transition-state fractionation factors are calculated for aldehyde reduction [φ(TS) = 0.83] and alcohol oxidation [φ(TS) = 0.70–1.08].

As pointed out previously (Klinman, 1976), the presence of an active-site functional group whose pK_a (8.25) is between the pK_a of aldehyde [pK_a ≈ -3 to -7 (Stewart et al., 1959)] and that of alcohol [pK_a ≈ 15 (Ballinger & Long, 1959)] would meet the requirements for concerted acid–base catalysis formulated by Jencks (1972). The magnitude of the solvent isotope effect for *p*-methoxybenzyl alcohol oxidation, k_{H₂O}/k_{D₂O} = 1.20 ± 0.09, rules out such a mechanism, however, since concerted acid–base catalysis is expected to be characterized

Scheme II: Mechanisms of Acid-Base Catalysis Compatible with the Observed Solvent Isotope Effects in the Yeast Alcohol Dehydrogenase Reaction^a



^a (A) Proton transfer from the active-site residue to aldehyde carbonyl, concomitant with a one-electron transfer, from coenzyme. (B) Displacement of metal-bound water, leading to inner-sphere complex formation between the active-site zinc and aldehyde carbonyl.

by $k_{\text{H}_2\text{O}}/k_{\text{D}_2\text{O}} \geq 2$ (Schowen, 1972, 1978). In contrast to alcohol oxidation, aldehyde reduction indicates a large inverse isotope effect, $k_{\text{H}_2\text{O}}/k_{\text{D}_2\text{O}} = 0.50 \pm 0.05$ for reduction by NADH. A threefold decrease in k_{cat} , which results from substitution of hydrogen by deuterium at C-4 of the dihydronicotinamide ring of NADH, leads to a similar isotope effect, $k_{\text{H}_2\text{O}}/k_{\text{D}_2\text{O}} = 0.58 \pm 0.06$. The dissimilarity between solvent isotope effects for alcohol oxidation and those for aldehyde reduction strongly suggests that an intermediate is formed in a fast step, prior to C-H cleavage, in the direction of aldehyde reduction. The inverse isotope effect observed upon formation of this intermediate is attributed to the loss of the unusual ground-state fractionation factor for the active-site functional group.

Two models are formally consistent with the observed inverse solvent isotope effects (Klinman et al., 1977; Klinman, 1978a). As illustrated in Scheme IIA acid-base catalysis involves a preequilibrium transfer of a proton to the carbonyl oxygen. Generation of a carbonium ion can be ruled out in light of the ~ 13 pK_a unit difference between the active-site residue and protonated aldehyde and the fact that the distribution of charge at C-1 of substrate in the transition state is equal to that of product alcohol. Consequently, the intermediate illustrated in Scheme IIA is the neutral protonated radical derived from a concomitant transfer of a proton plus one electron. In an alternative mechanism, Scheme IIB, the inverse isotope effect in the direction of aldehyde reduction results from a displacement of water from zinc by the carbonyl functional group of the aldehyde substrate, prior to the rate-determining hydrogen transfer step. Distinction between parts A and B of Scheme II for yeast alcohol dehydrogenase relies heavily on the available structural data for the horse liver enzyme. Several findings in the latter system implicate direct coordination of substrate to the active-site zinc. X-ray structural studies of the enzyme-NADH-dimethyl sulfoxide complex at 4.5-Å resolution (Eklund & Brändén, 1979), together with preliminary high-resolution data (Brändén et al., 1979), indicate that the oxygen of dimethyl sulfoxide undergoes direct coordination to zinc. Similar conclusions regarding direct coordination of oxygen from alcohols to zinc have also been reached from studies of abortive ternary complexes of enzyme-NADH-alcohol (Brändén et al., 1979).

Investigations of the mode of substrate/inhibitor binding in solution have led to conflicting results. Whereas nuclear

magnetic resonance studies of the effect of cobalt on the line width of either bound imidazole or isobutyramide have been interpreted in terms of second-sphere complexes (Young & Mildvan, 1977), the interaction of chromophoric aldehydes with horse liver alcohol dehydrogenase indicates red-shifted absorption maxima characteristic of inner-sphere complexes (Angelis et al., 1977). The available data are largely consistent with direct coordination of substrate oxygen to the active-site zinc in horse liver alcohol dehydrogenase, and by analogy, Scheme IIB is concluded to be the better representation for yeast alcohol dehydrogenase. An important distinction between yeast and horse liver alcohol dehydrogenases is that inner-sphere complexes are proposed to occur subsequent to the E·R·S complex in the yeast system, i.e., E·R·S' (Scheme IIB) does not reflect the most stable ground state in the direction of aldehyde reduction.

It is of interest to consider the contribution of hydrophobic factors to catalytic constants in the yeast alcohol dehydrogenase reaction in the context of Scheme IIB. Hydrophobic factors have previously been concluded to contribute to k_{cat} for the reduction of benzaldehydes vs. K_s for the oxidation of benzyl alcohols (Klinman, 1976), implicating different ground-state interactions for aldehyde and alcohol enzyme-bound substrates. The failure to detect a statistically significant contribution of hydrophobicity to k_{cat} for alcohol oxidation could, in principle, result from an extreme, alcohol-like transition-state structure. Alternatively, displacement of metal-bound water by the aldehyde carbonyl prior to the C-H cleavage step could be accompanied by a significant movement of the R functional group, giving rise to the observed hydrophobic component to k_{cat} for aldehyde reduction. In such a mechanism, Lewis acid activation of the effective substrate would be enhanced due to polarization of the carbonyl functional group in an environment characterized by increased hydrophobicity.

Recent studies by Schmidt et al. (1979) on the horse liver alcohol dehydrogenase reaction have allowed an estimate of the effect of D₂O on pre-steady-state transients for benzaldehyde reduction and benzyl alcohol oxidation. pH-dependent processes determined in their studies include both the dissociation and oxidation of benzyl alcohol from the enzyme-NAD⁺-benzyl alcohol ternary complex. In the case of alcohol release, $k_{\text{H}}/k_{\text{D}}$ is observed to vary from 1.15 at pH 6.0 to 0.39 at pH 10.2, consistent with little or no isotope effect on the limiting rate constant at low pH and a $\Delta\text{pK}_a \approx 0.3$ on the ionizing residue. In the case of benzyl alcohol oxidation, the solvent isotope effect was observed to be slightly inverse at all pH values: 0.68, 0.95, and 0.86 at pH 6.0, 7.0, and 8.75, respectively. The finding of an isotope effect close to 1 at high pH is analogous to our results with yeast alcohol dehydrogenase and indicates kinetic uncoupling of proton activation from C-H cleavage. The fact that $k_{\text{H}}/k_{\text{D}}$ is essentially pH invariant suggests little or no effect of D₂O on pK_a. Since the same functional group (pK_a = 6.4) has been concluded to control both alcohol release and oxidation from the enzyme-NAD⁺-alcohol complex, the lack of correspondence between the reported ΔpK_a values for these two processes is unexpected. More complete studies of solvent isotope effects for benzyl alcohol oxidation may help to resolve the apparent discrepancy in ΔpK_a .

The most interesting contrast between the horse liver and yeast systems concerns the solvent isotope effect on aldehyde reduction. Whereas we report inverse isotope effects on this process (Table V), Schmidt et al. (1979) have observed $k_{\text{H}_2\text{O}}/k_{\text{D}_2\text{O}} \approx 1$ for the horse liver system. An important

Table X: Summary of Kinetic Probes of Transition-State Structure in the Yeast Alcohol Dehydrogenase Catalyzed Reduction of Benzaldehydes

probe	magnitude of measured parameter	ref reaction
primary deuterium isotope effects ^a	$k_{\text{H}}/k_{\text{D}} = 3.0\text{--}5.4$	semiclassical maximum: 8–10
solvent deuterium isotope effects ^b	$k_{\text{H}_2\text{O}}/k_{\text{D}_2\text{O}} = 0.50$	$\phi(\text{GS}) = 0.35\text{--}0.54$ for the active-site functional group
structure–reactivity correlations ^c	$\rho^{\ddagger}(k_{\text{cat}}/K_{\text{m}}) = 1.2$	$\rho^{\ddagger}(K_{\text{eq}}) = 1.5$
α -secondary tritium isotope effects ^d	$k_{\text{H}}/k_{\text{T}} = 1.02$	$K_{\text{H}}/K_{\text{T}} = 0.75$

^a Klinman (1972, 1978b). ^b *p*-Methoxybenzaldehyde reduction by NADH (Tables V and IV). ^c Klinman (1976, 1972). ^d Benzaldehyde reduction by NADH (Tables VII and VI).

distinction between the two enzyme systems is the magnitude of $\text{p}K_{\text{a}}$ assigned to ZnOH_2 in the enzyme–NADH–aldehyde complex: $\text{p}K_{\text{a}} > 11$ for horse liver vs. $\text{p}K_{\text{a}} = 8.25$ for yeast alcohol dehydrogenase. In the case of the horse liver enzyme, zinc-bound water appears to be much more like free water ($\text{p}K_{\text{a}} = 15.7$) in its properties; consequently, displacement of water by substrate in a preequilibrium step would not be expected to be characterized by a significant solvent isotope effect. In addition, the high $\text{p}K_{\text{a}}$ of metal-bound water in the horse liver system may greatly facilitate inner-sphere complex formation, such that this complex contributes to K_{s} for the horse liver enzyme, in contrast to k_{cat} for yeast alcohol dehydrogenase.

Mode of C–H Cleavage. The available probes of transition-state structure in the yeast alcohol dehydrogenase reaction are summarized in Table X. Although primary deuterium isotope effects for benzaldehyde reduction are considerably less than the semiclassical maximum, there are considerable data to indicate that these values reflect the C–H bond cleavage step exclusively (Klinman, 1976, 1978a).

The relatively small magnitude of intrinsic primary isotope effects in dehydrogenase reactions has been discussed in the context of a formal hydride transfer mechanism (Klinman, 1978a). In the case of both proton and hydrogen atom transfer reactions, a bell-shaped relationship between primary hydrogen isotope effect and the overall thermodynamic properties of the reaction in question has been demonstrated: small isotope effects correlate with either a highly exo- [$\Delta G (\Delta H) \ll 0$] or endoenergetic [$\Delta G (\Delta H) \gg 0$] reaction, and maximum isotope effects with $\Delta G (\Delta H) \approx 0$ (Bell, 1974; More O'Ferrall, 1975; Pryor & Kneipp, 1971). To the extent that the thermodynamic property of a reaction determines the structure of the transition state (Hammond, 1955), these results are a corroboration of the Westheimer model, which predicts small primary isotope effects for early and late transition states and the semiclassical maximum when hydrogen is symmetrically placed between the donor and acceptor atoms (Westheimer, 1961). In the event that this model is independent of the mode of hydrogen activation (H^+ vs. $\text{H}\cdot$ vs. $\text{H}:$), the magnitude of primary isotope effects in the yeast alcohol dehydrogenase reaction suggests an asymmetric transition state resembling either the aldehyde or alcohol substrate.²

As discussed in detail previously, structure–reactivity correlations in the yeast alcohol dehydrogenase reaction indicate a distribution of charge at C-1 of substrate in the transition state which is unchanged relative to that of alcohol (Klinman, 1976). Although the absence of a significant charge development is consistent with a role for an active-site metal in acid–base catalysis of hydride transfer, an alternate mechanism could simply involve a late transition step in which hydride transfer from NADH to aldehyde is nearly complete. Simi-

larly, solvent isotope effects on aldehyde reduction indicate the near or complete loss of the unusual ground-state fractionation factor of an active-site residue (tentatively designated as ZnOH_2) at the transition state. In the preceding section, these effects have been discussed in the context of the formation of an inner-sphere complex between the aldehyde carbonyl and active-site zinc, prior to the hydrogen transfer step (Scheme IIB). In analogy with structure–reactivity correlations, an alternate mechanism could involve a late transition state resembling alcohol.

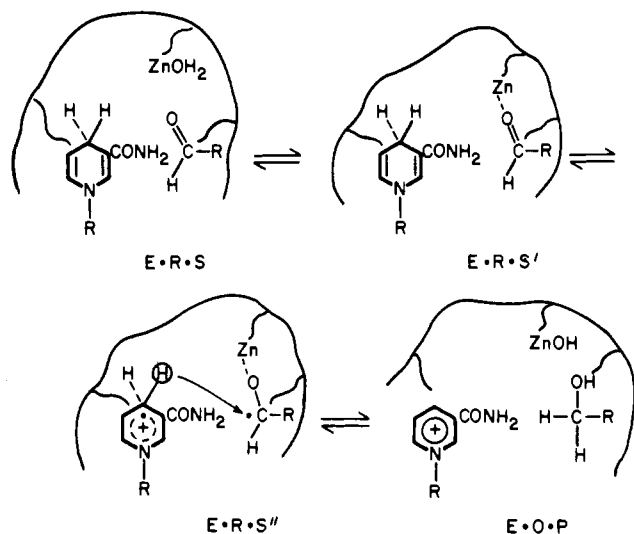
It should be pointed out that the magnitude of primary isotope effects is too large to be fully consistent with the very productlike transition-state structures required by structure–reactivity correlations and solvent isotope effects in the event of a single-step hydride transfer mechanism. Nonetheless, the above discussion points out the possible ambiguities in interpretation and the importance of multiple measurements of transition-state structure in a given reaction. The critical finding in the yeast alcohol dehydrogenase reaction regarding the mode of C–H cleavage is that the magnitude of α -secondary tritium isotope effects indicates a transition state characterized by the bond hybridization properties of aldehyde, in contrast to structure–reactivity correlations which indicate a transition state characterized by the charge properties of alcohol.

To the extent that changes in bond lengths and angles are expected to be coupled to changes in charge, it is not possible to reconcile this large discrepancy with a simple hydride transfer mechanism. If one permits the movement of electrons to become (partially) uncoupled from the transfer of the hydrogen nucleus, a range of transition-state structures varying in charge and bond rehybridization at C-1 is possible. In the extreme, one can write a radical mechanism in which aldehyde reduction is a two-step process involving a one electron transfer from NADH to aldehyde, followed by a rate-determining hydrogen atom transfer. Integrating the proposed mode of acid–base catalysis (Scheme IIB) into an overall mechanism, one obtains Scheme III; according to Scheme III, the enzyme reaction proceeds from the most stable ground state, $\text{E}\cdot\text{R}\cdot\text{S}$, through a series of increasingly activated intermediates, $\text{E}\cdot\text{R}\cdot\text{S}'$ (derived from displacement of metal-bound water by substrate) and $\text{E}\cdot\text{R}\cdot\text{S}''$ (derived from a one-electron transfer from NADH to metal-bound substrate). Hydrogen atom transfer from NADH^{\cdot} to the highly activated $\text{E}\cdot\text{R}\cdot\text{S}''$ is expected to occur through an early transition state involving little rehybridization of bonds at C-1.

The construction of Scheme III rests on the important assumption that the substrate-derived radical in $\text{E}\cdot\text{R}\cdot\text{S}''$ and the resultant transition state resemble alcohol with regard to charge properties and aldehyde with regard to bond hybridization properties. Studies of the effect of electronic substituent in hydrogen atom abstractions from ring-substituted toluenes indicate a stabilization of benzylic radical centers by electron-releasing groups, e.g., $\rho = -0.12$ to -0.52 for hydrogen abstraction by phenyl radicals [cf. Pryor et al. (1973) for a

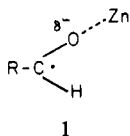
² These arguments assume a linear transition state for the transfer of hydrogen between two centers; bent transition states are predicted to have low primary isotope effects, independent of the symmetry of the transition state (More O'Ferrall, 1970).

Scheme III: Multistep Mechanism, Involving an Uncoupling of Electron from Hydrogen Atom Transfer, in the Reduction of Aldehydes by NADH^a

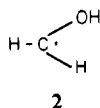


^a The reaction proceeds from the most stable ground state, E·R·S, through a series of activated intermediates: E·R·S', in which metal-bound water has been displaced by substrates, and E·R·S'', formed as the result of a one-electron transfer from NADH to metal-bound substrate.

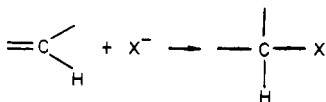
compilation of ρ values for hydrogen abstraction from toluenes under a variety of experimental conditions]. In the case of the formation of



from $R-CH_2OH$, the net ρ value will be the sum of ρ values for the generation of a benzylic radical ($\rho < 0$) and the generation of a partial negative charge on oxygen ($\rho > 0$). Although the latter effect is difficult to quantitate in the absence of data indicating the extent of delocalization of charge from oxygen to zinc, the observed lack of an electronic effect on alcohol oxidation can be attributed to a cancellation of equal but opposite ρ values. A quantitative estimate of the α -secondary isotope effect for the formation of radical **1** from $R-CHO$ could be made from the available force constants for C-H bending and stretching modes in the free radical derived from photolysis of methanol in argon and nitrogen matrices (Jacox & Milligan, 1973)



and formaldehyde (Cossee & Schachtschneider, 1966) by employing the Wolfsberg-Stern program for the calculation of isotope effects (Wolfsberg & Stern, 1964). The extensive calculations of Hartschorn & Shiner (1972) on small organic molecules indicate that the α -secondary isotope effect for the conversion of an sp^2 to an sp^3 center, e.g.



arises almost exclusively from the H-C-X bending motions in the sp^3 hybrid species. Since the transfer of one electron

to benzaldehyde would not introduce a new covalent bond, the magnitude of the α -secondary isotope effect for production of the radical in E·R·S'' from $R-CHO$ is expected to be quite small. In addition, comparison of the magnitude of α -secondary isotope effects for solvolysis reactions in which the transition state is predicted to be either carbonium ion like or alkene like indicates similar values (Shiner, 1971). Thus, geometric rather than charge constraints appear to be the dominant factor in determining α -secondary isotope effects, consistent with little or no equilibrium isotope effect in proceeding to a planar radical from an unsaturated carbon center.

A persistent problem in corroborating Scheme III is the failure to detect the presence of radical intermediates in NAD(P)H-dependent reactions by electron spin resonance. In addition, the premise that changes in bond reorganization and charge will be tightly coupled in the transition state may be faulty. Funderburk & Jencks (1978) have recently discussed the imbalance in values of Bronsted α 's and β 's, ρ values, and α -secondary isotope effects for the acid-catalyzed breakdown of carbinolamines to semicarbazones; as pointed out by these authors, secondary isotope effects indicate little or no bond rehybridization toward the sp^2 carbon atom in the transition state, in contrast to ρ values, which support a large degree of carbon-oxygen bond cleavage in the transition state. An examination of the correlation between electronic substituent effects and secondary isotope effects for the addition of nucleophiles to aldehydes under a variety of experimental conditions would provide important reference information toward the interpretation of the data in the yeast alcohol dehydrogenase reaction.³

A comparison of structure-reactivity correlations in the horse liver alcohol dehydrogenase to the yeast enzyme indicates a similar (possibly identical) distribution of charge at C-1 of substrate in the transition state (Hardman et al., 1974). Although α -secondary isotope effects have not yet been reported for the horse liver system, measurement of these effects would provide a subtle test of the extent to which transition-state structure has been conserved among enzymes from divergent evolutionary sources catalyzing the same reaction. In addition, detection of a closer correlation between the deduced charge distribution and bond hybridization at C-1 of substrate in the transition state of the horse liver alcohol dehydrogenase reaction could provide the necessary information to distinguish a concerted hydride transfer mechanism from the uncoupled radical reaction illustrated in Scheme III.

References

- Angelis, C. T., Dunn, J. F., Muchmore, D. C., & Wing, R. M. (1977) *Biochemistry* 16, 2922.
 Ballinger, P., & Long, F. A. (1959) *J. Am. Chem. Soc.* 81, 1050.
 Bell, R. P. (1974) *Chem. Soc. Rev.* 3, 513.
 Bernhard, S. A., Dunn, M. F., Luisi, P. L., & Schack, P. (1970) *Biochemistry* 9, 185.
 Brändén, C.-I., Eklund, H., Samama, J. P., & Wallén, L. (1979) XIth International Congress of Biochemistry, Toronto, Canada.
 Brooks, R. L., Shore, J. D., & Gutfreund, H. (1972) *J. Biol. Chem.* 244, 2382.

³ In a recent study, Young & McMahon (1979) report secondary isotope effects and substituent effects for the addition of HCN to substituted benzaldehydes. The magnitude of ρ^+ (which reflects the resonance interaction of substituents with the reacting center) and secondary isotope effects support similar transition-state structures for reaction in both water and 60% acetonitrile-40% water.

- Cossee, P., & Schachtschneider, J. H. (1966) *J. Chem. Phys.* **44**, 97.
- Dworschack, R. T., & Plapp, B. V. (1977) *Biochemistry* **16**, 2716.
- Eklund, H., & Brändén, C.-I. (1979) *J. Biol. Chem.* **254**, 3458.
- Eklund, H., Nordström, B., Zeppezauer, G.-S., Ohlsson, I., Boiwe, T., Söderburg, B.-O., Tapia, O., Brändén, C.-I., & Åkeson, Å. (1976) *J. Mol. Biol.* **102**, 27.
- Fukushima, S., & Reynolds, W. L. (1964) *Talanta* **11**, 283.
- Funderburk, L. H., & Jencks, W. P. (1978) *J. Am. Chem. Soc.* **100**, 6708.
- Hammond, G. S. (1955) *J. Am. Chem. Soc.* **77**, 334.
- Hardman, G. J., Blackwell, L. F., Boswell, C. R., & Buckley, P. D. (1974) *Eur. J. Biochem.* **50**, 113.
- Hartschorn, S. R., & Shiner, V. J., Jr. (1972) *J. Am. Chem. Soc.* **94**, 9002.
- Ho, T.-L., Ho, H. C., & Wong, C. M. (1972) *J. Chem. Soc., Chem. Commun.*, 791.
- Holzer, H., & Söling, H. D. (1962) *Biochem. Z.* **336**, 201.
- Jacox, M. E., & Milligan, D. E. (1973) *J. Mol. Spectrosc.* **47**, 148.
- Jencks, W. P. (1972) *Chem. Rev.* **72**, 705.
- Jörnvall, H., Eklund, H., & Brändén, C.-I. (1978) *J. Biol. Chem.* **253**, 8414.
- Katagiri, M., Takemori, S., Nakazawa, K., Suzuki, H., & Akagi, K. (1967) *Biochim. Biophys. Acta* **139**, 173.
- Klinman, J. P. (1972) *J. Biol. Chem.* **247**, 7977.
- Klinman, J. P. (1975) *Biochemistry* **14**, 2568.
- Klinman, J. P. (1976) *Biochemistry* **15**, 2018.
- Klinman, J. P. (1978a) in *Isotope Effects on Enzyme-Catalyzed Reactions* (Cleland, W. W., O'Leary, M. H., & Northrop, D. B., Eds.) p 176, University Park Press, Baltimore, MD.
- Klinman, J. P. (1978b) *Adv. Enzymol. Relat. Areas Mol. Biol.* **46**, 415.
- Klinman, J. P. (1980) *CRC Crit. Rev. Biochem.* (in press).
- Klinman, J. P., Welsh, K. M., & Creighton, D. J. (1977) *Alcohol and Aldehyde Metabolizing Systems* (Thurman, R. G., Williamson, J. R., Drott, H. R., & Chance, B., Eds.) Vol. II, p 53, Academic Press, New York.
- Kvassman, J., & Pettersson, G. (1976) *Eur. J. Biochem.* **69**, 279.
- Kvassman, J., & Pettersson, G. (1978) *Eur. J. Biochem.* **87**, 417.
- Laughton, P. M., & Robertson, R. E. (1969) in *Solute Solvent Interactions* (Coetzee, J. F., & Ritchie, C. D., Eds.) p 400, Marcel Dekker, New York.
- Lowry, O. J., Rosebrough, N. J., Farr, A. L., & Randall, R. J. (1951) *J. Biol. Chem.* **193**, 265.
- McFarland, J. T., & Chu, Y.-H. (1975) *Biochemistry* **14**, 1140.
- Melander, L. (1960) *Isotope Effects on Reaction Rates*, Ronald Press, New York.
- More O'Ferrall, R. A. (1970) *J. Chem. Soc. B*, 785.
- More O'Ferrall, R. A. (1975) in *Proton Transfer Reactions* (Caldin, E. F., & Gold, V., Eds.) p 201, Chapman and Hall, London.
- Pryor, W. H., & Kneipp, K. G. (1971) *J. Am. Chem. Soc.* **93**, 5584.
- Pryor, W. A., Lin, T. J., Stanley, J. P., & Henderson, R. W. (1973) *J. Am. Chem. Soc.* **95**, 6993.
- Racker, E. (1950) *J. Biol. Chem.* **184**, 313.
- Rafter, G. W., & Colowick, S. P. (1957) *Methods Enzymol.* **3**, 887.
- Schmidt, J., Chen, J., De Traglia, M., Minkel, O., & McFarland, J. T. (1979) *J. Am. Chem. Soc.* **101**, 3034.
- Schowen, R. L. (1972) *Prog. Phys. Org. Chem.* **9**, 275.
- Schowen, R. L. (1978) in *Isotope Effects on Enzyme-Catalyzed Reactions* (Cleland, W. W., O'Leary, M. H., & Northrop, D. B., Eds.) p 64, University Park Press, Baltimore, MD.
- Seebach, D., Erikson, B. W., & Singh, G. (1966) *J. Org. Chem.* **31**, 4303.
- Shiner, V. J., Jr. (1971) in *Isotope Effects in Chemical Reactions* (Collins, C. J., & Bowman, N. S., Eds.) p 107, Van Nostrand-Reinhold, New York.
- Shore, J. D., & Gutfreund, H. (1970) *Biochemistry* **9**, 4655.
- Splinter, R. C., Harris, S. J., & Tobias, R. S. (1968) *Inorg. Chem.* **7**, 897.
- Stewart, R., Gatzke, A. L., Macke, M., & Yates, K. (1959) *Chem. Ind. (London)*, 331.
- Suhara, K., Takemori, S., & Katagiri, M. (1969) *Arch. Biochem. Biophys.* **130**, 422.
- Swain, C. G., Stivers, E. C., Reuwer, J. F., Jr., & Schaad, L. J. (1958) *J. Am. Chem. Soc.* **80**, 5885.
- Westheimer, R. H. (1961) *Chem. Rev.* **61**, 265.
- Wolfsberg, M., & Stern, M. J. (1964) *Pure Appl. Chem.* **8**, 225.
- Young, J. M., & Mildvan, A. S. (1977) in *Alcohol and Aldehyde Metabolizing Systems* (Thurman, R. G., Williamson, J. R., Drott, H. R., & Chance, B., Eds.) Vol. II, p 109, Academic Press, New York.
- Young, P. R., & McMahan, P. E. (1979) *J. Am. Chem. Soc.* **101**, 4678.